Sound transmission through a double leaf partition with edge flanking
Craik, R. J. M.; Nightingale, T. R. T.; Steel, J. A.

Publisher's version / Version de l'éditeur:

Journal of the Acoustical Society of America, 101, February 2, pp. 964-969, 1997-02-01

Sound transmission through a double leaf partition with edge flanking

NRCC-41501

Craik, R.J.M.; Nightingale, T.R.T.; Steel, J.A.

February 1997

A version of this document is published in / Une version de ce document se trouve dans:
Journal of the Acoustical Society of America, 101, (2), February, pp. 964-969, February 01, 1997

Sound transmission through a double leaf partition with edge flanking

R. J. M. Craik
Department of Building Engineering and Surveying, Heriot-Watt University, Riccarton, Edinburgh EH14 4AS, United Kingdom

T. R. T. Nightingale
Acoustics Laboratory, Institute for Research in Construction, National Research Council Canada, Ottawa, Ontario K1A 0R6, Canada

J. A. Steel
Department of Mechanical and Chemical Engineering, Heriot-Watt University, Riccarton, Edinburgh EH14 4AS, United Kingdom

(Received 8 January 1996; revised 2 September 1996; accepted 24 September 1996)

Lightweight double leaf partitions are widely used and with proper design give good sound isolation. However, when these walls are used as party walls between dwellings, then precautions are necessary to prevent the transmission of fire and smoke. This is usually carried out by placing a firestop in the cavity. This firestop introduces flanking transmission paths reducing the airborne transmission loss of the wall. A simple model is developed which can predict vibration transmission across this type of structural connection. The structural vibration transmission loss can then be used with a more general statistical energy analysis model to give the sound transmission through the entire system. Predicted airborne transmission loss results for a variety of different materials are compared with measured results and good agreement is obtained. © *1997 Acoustical Society of America.* [S0001-4966(97)01002-3]

PACS numbers: 43.55.Ti, 43.55.Rg, 43.55.Vj [JDQ]

INTRODUCTION

Double walls are widely used both as internal partitions and as high performance walls separating two different dwellings. They normally consist of a frame of wood or profiled metal channel covered with one or more layers of gypsum board. If the wall is to have good sound isolating properties, then there will usually be sound absorbing material in the cavity which will increase the airborne transmission loss. Sound insulation will be further improved if two separate frames are used to support the gypsum board so that there is no physical connection between the two leaves of the wall. It is these high performance walls that are considered in this paper.

When properly designed these partitions work well and give good sound isolation. However, in walls that separate dwellings, fire and smoke must also be considered as the cavity can allow the spread of fire throughout the dwelling. To prevent this, a physical barrier called a firestop is usually placed in the cavity as shown in Fig. 1. Typical materials used are plywood, gypsum board, or steel.[1] When the firestop is at floor level (as shown in Fig. 1) the simplest method of construction is to make the plywood floor deck continuous under the wall. When the firestop is a vertical edge (in which case Fig. 1 is a plan rather than a section and the floor is another wall), then the gypsum board that covers the flanking wall can be continuous across the cavity of the separating wall.

Measurements made in real buildings show that the airborne transmission loss of a wall when a firestop has been fitted is less than when there is no firestop. This is confirmed by laboratory measurements made on standard forms of construction.[2]

In this paper a model is developed which enables the vibration transmission across a continuous firestop to be predicted. The predicted structural transmission loss results from this model are then used within a more general statistical energy analysis framework. This enables noise transmission between the two rooms through the partition system and also across the firestop to be determined.

A comparison of measured results with these calculations shows good agreement. It is shown that there are considerable differences in sound transmission depending on which firestop materials are used and that this difference can be predicted. The model enables appropriate firestop materials to be selected.

I. THEORY OF STRUCTURE-BORNE TRANSMISSION

The actual construction of the joint between the two leaves of the wall and the two parts of the floor at the firestop is complex and some simplifications are necessary if useable models are to be developed. A floor will usually consist of wood joists with a floor covering (typically a plywood deck) and a gypsum board ceiling. Each leaf of the wall will generally have a metal or wooden frame with gypsum board covering. For simplicity, the effects of the joists in the floor and the frame in the walls have not been considered. Their omission greatly simplifies the calculation but can lead to some errors.

In the test structure the frame reduced vibration propagation across both the gypsum board wall and the plywood

 0001-4966/97/101(2)/964/6/$10.00

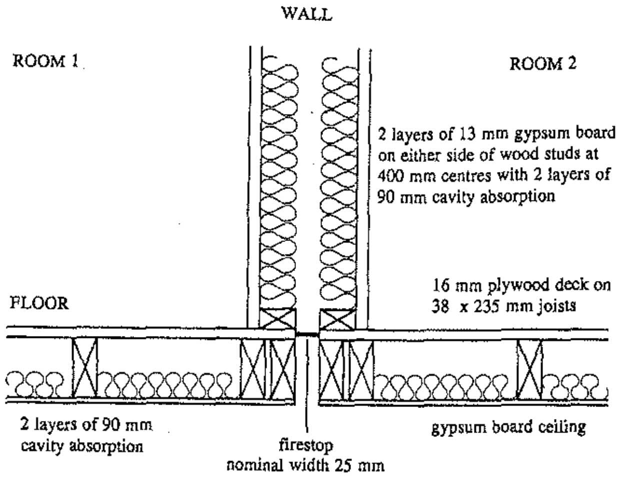

FIG. 1. Section through a double wall resting on a wood floor with a firestop to prevent the passage of fire and smoke.

floor. If a panel is excited by airborne sound then the vibration energy will be uniformly distributed across the panel and there will be no net power flow between different sections so that the effect of the frame will be negligible. However, in flanking paths the excitation of the receiving room wall and floor is along an edge. In this case the effect of the frame and the joists will be more important. In the test constructions the joists were parallel to the test joint and so affected the propagation of energy away from the joint. In the walls (both the common wall and the flanking wall) the frame members were vertical. If the firestop element is at floor level then the wall frame will have a small effect on the distribution of energy across the panel. If the firestop is a vertical edge then the effect will be larger.

Another approximation that simplifies the calculations is to ignore in-plane vibration. Where a floor and a wall meet at a right angle it is reasonable, as a first approximation, to assume that each will prevent lateral motion of the other. Thus, the floor will prevent in-plane motion of the wall that is at right angles to it and *vice versa*. The wall and floor are still free to rotate but there is no lateral motion of the actual joint. This assumption prevents the generation of in-plane displacements and power is then transmitted by moments only. With these assumptions the structural transmission at the joint can be determined.

The parameter used to describe transmission is the transmission coefficient, τ, defined as the ratio of the power transmitted across a joint to the power incident on it. This is then related to the structural transmission loss, $H=10\log(1/\tau)$.

The method commonly used to determine the structural transmission loss at the joints between plates is to examine the behavior of semi-infinite plates connected at a joint.[3] In this case there are four plates (two walls and two floors). It is assumed that there is a bending wave incident on the joint and that the objective of the analysis is to calculate the amplitude of the waves leaving the joint and hence the structural transmission loss. This is a standard procedure for calculating structural transmission loss.[3,4]

The general coordinate system used for the calculations is shown in Fig. 2. On each plate there will be a traveling

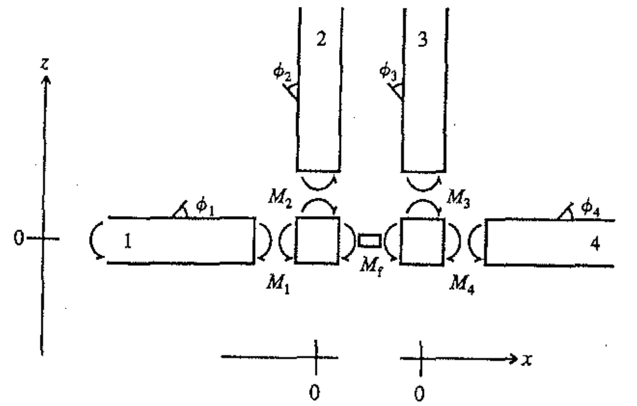

FIG. 2. Coordinate system used to calculate the structural transmission loss.

bending wave with amplitude T and a near-field bending wave with amplitude T_n. In addition on plate 1 there is assumed to be a wave incident on the joint with unit amplitude. The displacement on plates 1–4 (ξ_1 to ξ_4) can then be given as

$$\xi_1=(e^{-ik_1\cos\theta_1 x}+T_1e^{ik_1\cos\theta_1 x}+T_{n1}e^{k_{n1}x})\times e^{-ik_1\sin\theta_1 y}e^{i\omega t},\tag{1}$$

$$\xi_2=(T_2e^{-ik_2\cos\theta_2 z}+T_{n2}e^{-k_{n2}z})e^{-ik_2\sin\theta_2 y}e^{i\omega t},\tag{2}$$

$$\xi_3=(T_3e^{-ik_3\cos\theta_3 z}+T_{n3}e^{-k_{n3}z})e^{-ik_3\sin\theta_3 y}e^{i\omega t},\tag{3}$$

$$\xi_4=(T_4e^{-ik_4\cos\theta_4 x}+T_{n4}e^{-k_{n4}x})e^{-ik_4\sin\theta_4 y}e^{i\omega t},\tag{4}$$

where k is the wave number.

Since power is transmitted only by moments in this model the orientation of the plates can be changed without affecting the structural transmission loss. Thus, the numbering can be changed so that plate 1 is the wall and plate 2 is the floor. The only necessary assumption is that plates 1 and 2 are on one side of the firestop and that 3 and 4 are on the other.

If the sound field on plate 1 is diffuse then all angles of incidence are possible. For a given angle of incidence θ_1 (measured from the normal) on plate 1 the angle of transmission of the other waves can be found from the relationship

$$k_1\sin\theta_1=k_2\sin\theta_2=k_3\sin\theta_3=k_4\sin\theta_4.\tag{5}$$

k_n is the near-field wave number in the x or z direction and can be found for any plate from[3]

$$k_{ni}=\sqrt{k_i^2+k_i^2\sin^2\theta_i}.\tag{6}$$

The requirement that the displacement of all the plates be zero at the boundary (where x and $z=0$) gives, from Eqs. (1)–(4),

$$1+T_1+T_{n1}=T_2+T_{n2}=T_3+T_{n3}=T_4+T_{n4}=0,\tag{7}$$

so that the amplitude of the near-field waves can be given in terms of the traveling wave amplitude for each plate.

At the boundary it is assumed that the plates on the left of the joint and those on the right are rigidly bonded together so that the angle between them is preserved. This leads to two equations linking the slope, ϕ, on plates 1 and 2 and the slopes on plates 3 and 4. Equating the slopes on plates 1 and 2 gives $\phi_1=\phi_2$. Expressing the slope as the derivative of the displacement[3] gives

$$\frac{\partial \xi_1}{\partial x}=\frac{\partial \xi_2}{\partial z}. \tag{8}$$

Evaluating this at the origin where x, and $z=0$ gives

$$T_1[-k_{n1}+ik_1\cos\theta_1]+T_2[-k_{n2}+ik_2\cos\theta_2]$$
$$=k_{n1}+ik_1\cos\theta_1. \tag{9}$$

Similarly, equating the slopes of plates 3 and 4, so that $\phi_3=\phi_4$, gives

$$\frac{\partial \xi_3}{\partial z}=\frac{\partial \xi_4}{\partial x}, \tag{10}$$

which can be given as

$$T_3[k_{n3}-ik_3\cos\theta_3]+T_4[-k_{n4}+ik_4\cos\theta_4]=0. \tag{11}$$

Two other equations can be written relating the moments. Summing the moments about each side in turn and using the coordinate system shown in Fig. 2 gives

$$M_1-M_2-M_f=0 \tag{12}$$

and

$$M_3+M_4-M_f=0, \tag{13}$$

where M_i is the moment acting on the firestop from plate i and M_f is the moment acting on the plates due to the firestop.

The moment (per unit width) acting on the boundary due to wave motion on a plate can be given by[3]

$$M=-B\left[\frac{\partial^2\xi}{\partial x^2}+\mu\frac{\partial^2\xi}{\partial y^2}\right], \tag{14}$$

so that, by substituting the displacement into Eq. (14) and evaluating at x, y and $z=0$, the moment due to each plate can be found. For moments on plates 2 and 3 the x dependence in Eq. (14) is changed to z. Here, B is the material stiffness per unit width and is given in terms of Young's modulus E, the thickness h, and Poisson's ratio μ, as

$$B=\frac{Eh^3}{12(1-\mu^2)}. \tag{15}$$

The moment (per unit width) acting on the plates due to the firestop can be written in terms of the change in slope across its width $(\phi_1-\phi_4)$ and the stiffness (per unit width) of the firestop component. This depends on both the stiffness of the firestop material B_f and the cavity depth d to give

$$M_f=\frac{B_f}{d}(\phi_1-\phi_4), \tag{16}$$

where d, the width of the firestop, is taken as the separation between the sole plates of the wall (25 mm for the test structure). At normal incidence the bending stiffness of the firestop can be found from Eq. (15). At other angles of incidence there also will be bending along the y axis which will increase the overall stiffness. Accounting for this more correctly would increase the overall complexity of the model and is not justified, given the other approximations and assumptions that have been made. Therefore in all calculations the simple approximation of Eq. (15) has been used.

Inserting Eqs. (14) and (16) into Eqs. (12) and (13), and substituting for the displacement, gives the two moment equations as

$$T_1[2B_1k_1^2+B_fk_{n1}/d-iB_fk_1\cos\theta_1/d]+T_2[-2B_2k_2^2]$$
$$+T_4[B_fk_{n4}/d-iB_fk_4\cos\theta_4/d]$$
$$=-2B_1k_1^2-B_fk_{n1}/d-iB_fk_1\cos\theta_1/d \tag{17}$$

and

$$T_1[B_fk_{n1}/d-iB_fk_1\cos\theta_1/d]+T_3[2B_3k_3^2]$$
$$+T_4[2B_4k_4^2+B_fk_{n4}/d-iB_fk_4\cos\theta_4/d]$$
$$=-B_fk_{n1}/d-iB_fk_1\cos\theta_1/d. \tag{18}$$

The four equations, (9), (11), (17), and (18), can be solved numerically to give the amplitude of the waves leaving the joint from which the structural transmission coefficient τ can be found using

$$\tau_{12}(\theta)=\frac{\rho_{s2}k_1\cos\theta_2|T_2|^2}{\rho_{s1}k_2\cos\theta_1}, \tag{19}$$

where ρ_s is the surface density.

The angular averaged transmission coefficient can then be found from[3]

$$\tau_{av}=\int_0^{\pi/2}\tau(\theta)\cos\theta\,d\theta. \tag{20}$$

As the four plates that make up the joint are often very similar a useful approximation is to assume that all the plates are made from the same materials and have the same thickness. In this case, the normal incidence solution for the structural transmission loss can be given as

$$H_{13}=H_{14}=10\log\left[\frac{16B^2k^2d^2}{B_f^2}+\frac{16Bkd}{B_f}+8\right]. \tag{21}$$

This can be used to give an estimate of the structural transmission loss and can be used to quickly rank different materials.

The relation between the parameter Bkd/B_f and the structural transmission loss can be seen in Fig. 3 for the case where all four plates are assumed to have the same material properties. The results show both the random incidence solution and the normal incidence approximation. It can be seen that the normal incidence approximation is about 2 dB less than the random incidence solution. At low frequencies or for stiff firestops (the left of Fig. 3) the structural transmission loss tends to a constant value. The limits are 9 dB for the normal incidence solution and 10.8 dB for the random incidence solution and are the same as the result for a rigid cross joint. As the frequency increases or the stiffness gets less so the structural transmission loss increases.

The solution given above is for four plates connected at a joint. In some cases there may be additional plates if for example the walls under the floor were included. For each

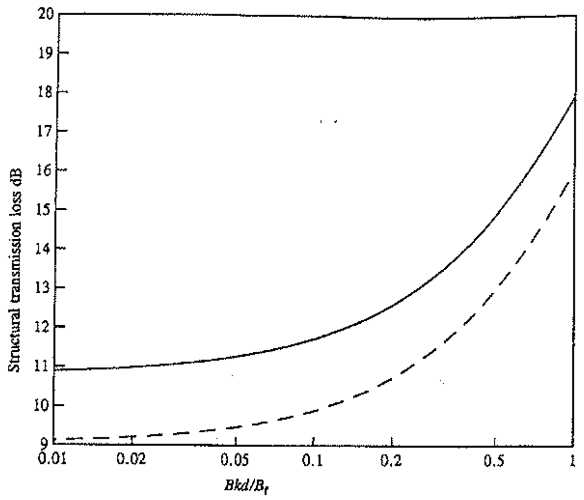

FIG. 3. Structural transmission loss between plates 1 and 3 (or 4) at a joint where all the plates are made from the same material and have the same thickness. ———, random incidence; ----, normal incidence.

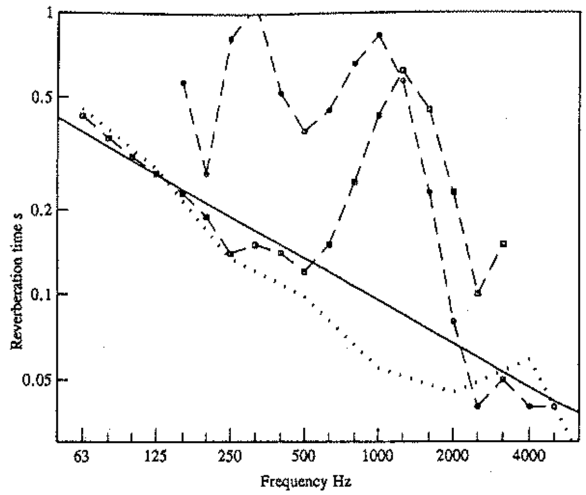

FIG. 4. Reverberation time measured in the cavity of the double wall and floor. --□--, measured in the wall; --O--, measured in the floor; ———, estimated curve $3/\sqrt{f}$; ...., measured in an isolated cavity.

additional plate there is one additional equation relating the slope of the new plate to an existing plate and one additional term in one of the moment equations.

II. TEST FACILITY

In order to test the theory given in the previous section measurements were carried out in the flanking laboratory of the National Research Council of Canada.[2] The test facility consists of four rooms (two up and two down) with volumes from 35 to 50 m^3. The test joint shown in Fig. 1 formed the only link between two pairs of otherwise separate rooms. The walls were made from wood frames covered with two layers of gypsum board and the floors were constructed from 38- ×235-mm joists with 16-mm plywood on the top and 2 layers of 13-mm gypsum board on the ceiling attached using resilient furring strips. The separating wall (13.5 m^2) had independent frames with two layers of plasterboard on each side and the cavity between the two leaves was filled with sound absorbing material.

Sound transmission was measured between the upper pairs of rooms and the firestop was either at floor level or at a wall edge. When the firestop was at floor level the joint is like that shown in Fig. 1, except that there are rooms underneath. Due to the method of construction it was not appropriate to include the walls below the floor in the analysis, as there was no significant physical connection between the floor assembly and the lower party wall.

Sound transmission between the test rooms was predicted using a statistical energy analysis model. Statistical energy analysis modeling is described in more detail by Craik[4] and details of the model used are given in Ref. 5.

The firestops used were all 25 mm wide and were 0.38-mm steel, 16-mm plywood or 26-mm gypsum board (made from 2 sheets of 13-mm gypsum board).

III. RESULTS

All of the tests carried out were of airborne sound transmission between two rooms separated by a test wall, as shown in Fig. 1 but with additional rooms underneath. A noise source was placed in room 1 and a standard sound transmission test[6] was carried out to give the airborne transmission loss of the wall.

The first tests were carried out when there was no firestop connecting the two leaves of the separating wall so that direct transmission through the wall together with any minor flanking paths through the rest of the laboratory could be determined.

As the dominant transmission path is the direct path through the wall, the absorption in the cavity is important. Transmission through the double wall can be considered as transmission into the cavity followed by transmission out of the cavity. The sound-pressure level in the cavity is inversely proportional to the cavity damping so that the overall airborne transmission loss is inversely proportional to the reverberation time of the cavity.

The reverberation time, T, that was measured in the wall cavity and in one of the floor cavities can be seen in Fig. 4. The reverberation time was much less than would be expected for a normal room and was very difficult to measure. A standard decay rate method was used with a small loudspeaker placed in the cavity. There was considerable interference in the cavity decay curve from energy returning from the rooms and the rest of the structure making the decay curves difficult to interpret. It was assumed that the high readings of around 0.5 s were due to the reverberation time of the rooms and that the true reverberation time was the lowest of the measured readings. A best fitting estimate of $T=3/\sqrt{f}$ was therefore used as this passed through the lowest readings. Subsequent measurements were made on an isolated test structure that reproduced the conditions in the cavity without interference from any surrounding structure. The results for the isolated cavity (also shown in Fig. 4) confirm that the estimate is a good one.

Using these data and a standard SEA model, sound transmission through the basic partition was predicted. This is shown together with the measured airborne transmission loss in Fig. 5. It can be seen that there is good agreement

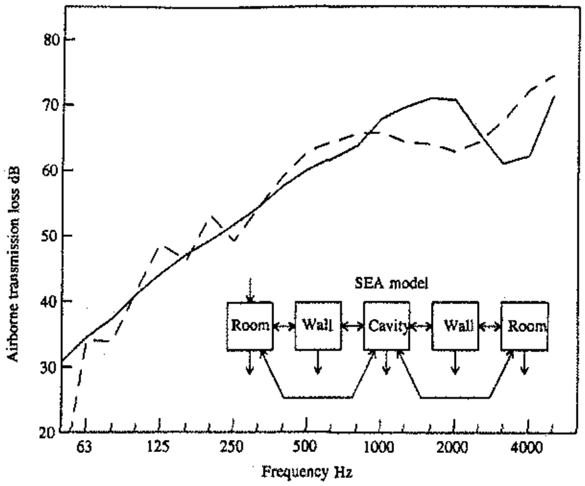

FIG. 5. Airborne transmission loss of a double wall with no firestop. A simplified SEA model is shown in the insert. ———, predicted; ----, measured.

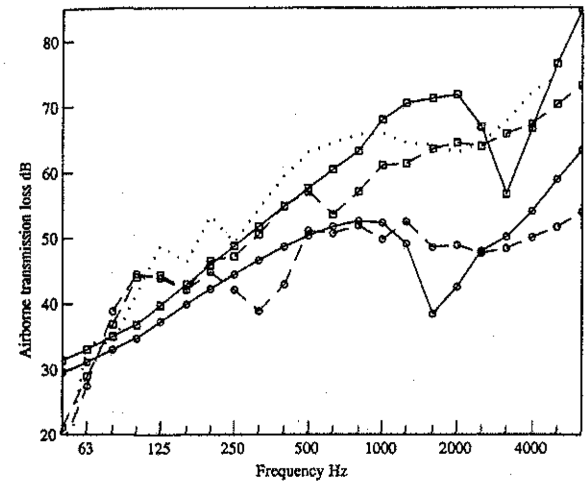

FIG. 6. Airborne transmission loss for a wall with a steel and a plywood firestop at floor level. --□--, measured with a steel firestop; ——□——, predicted with a steel firestop; --○--, measured with a plywood firestop; ——○——, predicted with a plywood firestop; ...., measured with no firestop.

between the measured and predicted data, although the predicted dip at around 3 kHz associated with the critical frequency is not at the correct frequency. The SEA model used included all of the surrounding structure (using 20 subsystems) and is therefore more complex than the 5 subsystem model shown in the insert. However, the 5 subsystem model describes the direct paths through the partition and is sufficient for most purposes. In the SEA model the arrows from the room to the cavity represent the nonresonant (mass-law) transmission path and will dominate transmission at frequencies below the critical frequency.

Using the 5 subsystem model the airborne transmission loss due to the direct path can be given as[4]

$$R = R_1 + R_2 + 10 \log \frac{1}{f T_c} + 14.4, \tag{22}$$

where R is the overall airborne transmission loss, $R_{1,2}$ is the airborne transmission loss of the individual leaves of the wall and can be approximated to the mass-law equation[7] below the critical frequency, and T_c is the reverberation time of the cavity. This equation assumes that the cavity is sufficiently narrow that it behaves as a two dimensional space. f is the band center frequency (usually $\frac{1}{3}$ octaves).

When the firestop is introduced then sound is transmitted by additional paths which decrease the overall airborne transmission loss. The model is then much more complex and there is no single simple algebraic expression for the sound reduction index equivalent to Eq. (22). Either a full SEA model has to be set up or else a path by path analysis carried out.[4] The results of such calculations can be seen in Fig. 6, which shows the measured results for no firestop (shown in Fig. 5) together with the measured and predicted results for situations where there is a steel firestop and a plywood firestop at floor level.

At low frequencies sound is mainly transmitted via the direct paths so that the additional flanking paths through the firestop make little difference. At higher frequencies the results show clearly the effect of the additional flanking paths. The steel firestop provides very weak coupling and gives results that are more or less the same as the results for no firestop. The results for the plywood firestop show a significant decrease in airborne transmission loss at the higher frequencies. This result shows that the best method of reducing flanking is to use a flexible firestop such as a thin steel plate.

An analysis of the different transmission paths associated with transmission between the two rooms when there is a plywood firestop can be seen in Fig. 7. The figure shows the predicted airborne transmission loss when there is no firestop together with the four main paths associated with the firestop. The least important is the path from source room to the wall in the source room across the firestop to the wall in the receiving room followed by radiation into the receiving room. The most important of the flanking paths is from the source room, into the floor of the source room, across the joint into the floor of the receiving room, followed by radiation into the receiving room. The other two flanking paths

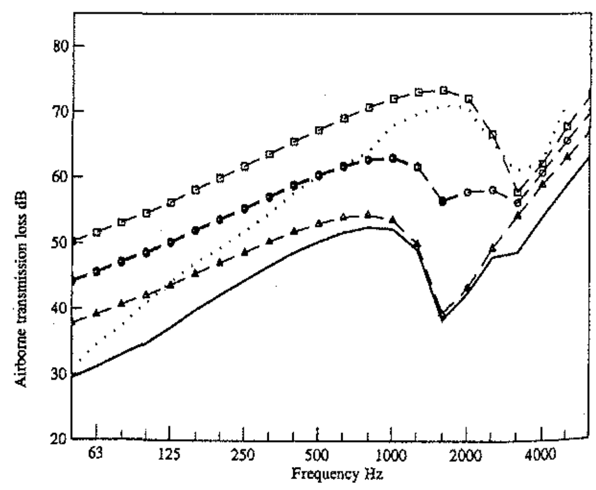

FIG. 7. Transmission paths associated with the plywood firestop. ———, sum of all paths; --□--, wall–wall path; --○--, wall-floor path; --○--, floor–wall path; --△--, floor-floor path; ...., prediction with no firestop.

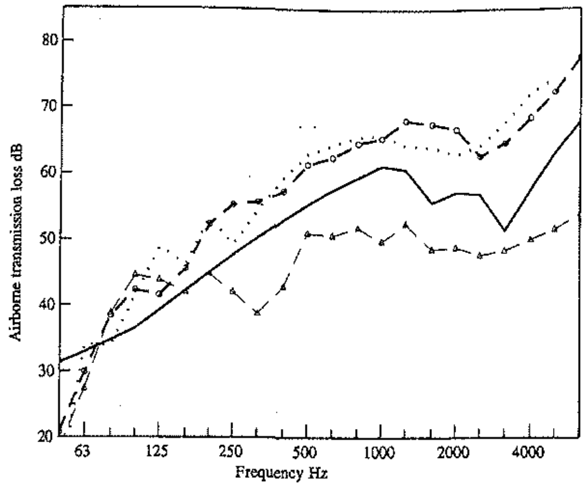

FIG. 8. Airborne transmission loss for transmission between the two rooms when a floating floor is placed over the floor to reduce excitation of and radiation from the floor. ...., measured with no firestop; —O—, measured with a plywood firestop and a floating floor; —Δ—, measured with a plywood firestop; ———, predicted.

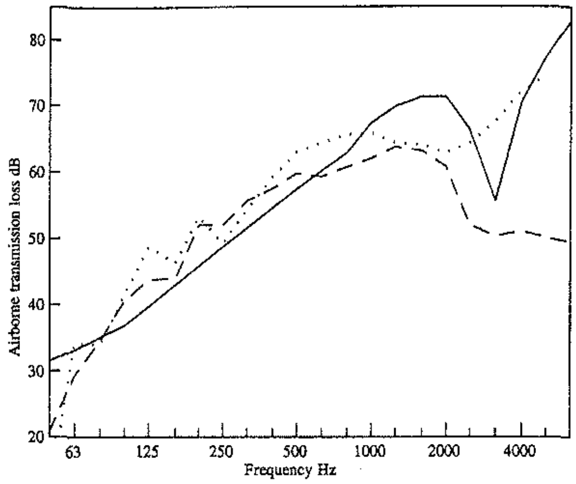

FIG. 9. Airborne transmission loss of the double wall when there is a gypsum board firestop providing flanking along the external wall. -----, measured; ———, predicted; ...., measured with no firestop.

from the source room wall to the receiving room floor and from the source room floor to the receiving room wall are approximately equal and lie midway between the other two flanking curves. As was shown in the measured data in Fig. 6, the transmission at low frequencies is dominated by the direct path through the wall. In this figure the prediction for the wall with no firestop is shown for comparison. At the higher frequencies, above about 125 Hz, the dominant path is the flanking path involving transmission from one floor to the other and shows clearly the effect of this path on transmission between the two rooms.

Given that the dominant flanking path involves the floor in each room then one method of improving the overall transmission loss between the two rooms would be to place a floating floor on top of the structural floor to reduce excitation of the floor and radiation from it. The results for such a floor can be seen in Fig. 8. This shows the measured and predicted results for the case where there is a floating floor on the receiving side only. For simplicity it was assumed that the floating floor only eliminated coupling between the floor and the room (effectively eliminating two of the four main flanking paths). The predicted results are lower than the measured results but both show a significant increase in the airborne transmission loss compared to that for a plywood firestop.

Figure 9 shows results for flanking along the external wall where the firestop was two sheets of gypsum board carried through from the wall of one room to the wall of the other. Again the results are shown for a system with and without a firestop. In this case the firestop has little effect except at the higher frequencies.

IV. CONCLUSIONS

Despite the simplicity of the model used for the calculation of structural transmission loss, it gives reasonable agreement between the measured and predicted results. The theory predicts the correct trends and therefore allows a comparison of the effect of different firestop materials. The plywood firestop is the simplest method of forming a firestop at floor level and leads to significant flanking paths for double partition constructions. In the test construction these could be reduced by placing a floating floor on top of the structural floor. Alternatively a thin steel sheet can be used as a firestop to minimise flanking transmission.

An estimate of the structural transmission loss can be found from Eq. (21) which can be used to rank different test materials.

[1] National Building Code of Canada 1990, Part 9, Section 9.10.15 Firestops, Associate Committee on the National Building Code, National Research Council, Canada, 1991.

[2] T. R. T. Nightingale, "Methods for measuring and identifying flanking transmission in wood-framed constructions," Proc. INTERNOISE **93**, 953–956 (1993).

[3] L. Cremer, M. Heckl, and E. E. Ungar, *Structure-Borne Sound* (Springer-Verlag, Berlin, 1988).

[4] R. J. M. Craik, *Sound Transmission Through Buildings Using Statistical Energy Analysis* (Gower, Aldershot, United Kingdom, 1996).

[5] R. J. M. Craik, J. A. Steel, and T. R. T. Nightingale, "Sound transmission through framed buildings," IRC internal report IRC-IR-672, Institute for Research in Construction, National Research Council, Ottawa, Canada, 1995.

[6] ASTM E336-90, "Standard test method for measurement of airborne sound insulation in buildings," 1995 (also ISO 140 1978).

[7] L. L. Beranek and I. L. Ver, *Noise and Vibration Control Engineering* (Wiley, New York, 1992).